Supplementary Information for "Engineering magnetic topological insulators in $Eu_5M_2X_6$ Zintls"

Nicodemos Varnava,[1,*] Tanya Berry,[2,3,4] Tyrel M. McQueen,[2,3,4] and David Vanderbilt[1]

[1] *Department of Physics & Astronomy, Rutgers University, Piscataway, New Jersey 08854, USA*
[2] *Institute for Quantum Matter and William H. Miller III Department of Physics and Astronomy, The Johns Hopkins University, Baltimore, Maryland 21218, USA*
[3] *Department of Chemistry, The Johns Hopkins University, Baltimore, Maryland 21218, USA*
[4] *Department of Materials Science and Engineering, The Johns Hopkins University, Baltimore, Maryland 21218, United States*

I. BAND STRUCTURE OF $Eu_5In_2Sb_6$ IN THE PUTATIVE IN-PLANE A-TYPE AFM ORDER

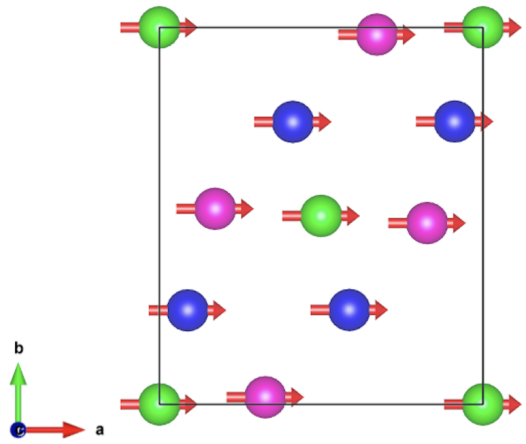

Supplementary Figure 1. In-plane ferromagnetic configuration for the 10 Eu in the $z = 0$ plane. There are three symmetry independent Eu atoms with Wyckoff positions $4g$ (blue), $4g$ (purple) and $2a$ (green). The A-type AFM configuration can be constructed by doubling the unit cell along the c-axis and flipping the spins on the $z = 1/2$ plane so that there is no net magnetization.

In Supplementary Fig. 2 we compare the band structure of $Eu_5In_2Sb_6$ for different values of U with and without SOC when the in-plane A-type AFM configuration is assumed. In the absence of SOC, the band overlap decreases as the U value is increased moving the compound closer to the CET limit. For the range of U values considered the topological index remains unaffected. Note that in this work, we take $U = 5$eV based on previous studies of compounds with Eu^{2+}[1–3].

* Corresponding author; nvarnava@physics.rutgers.edu

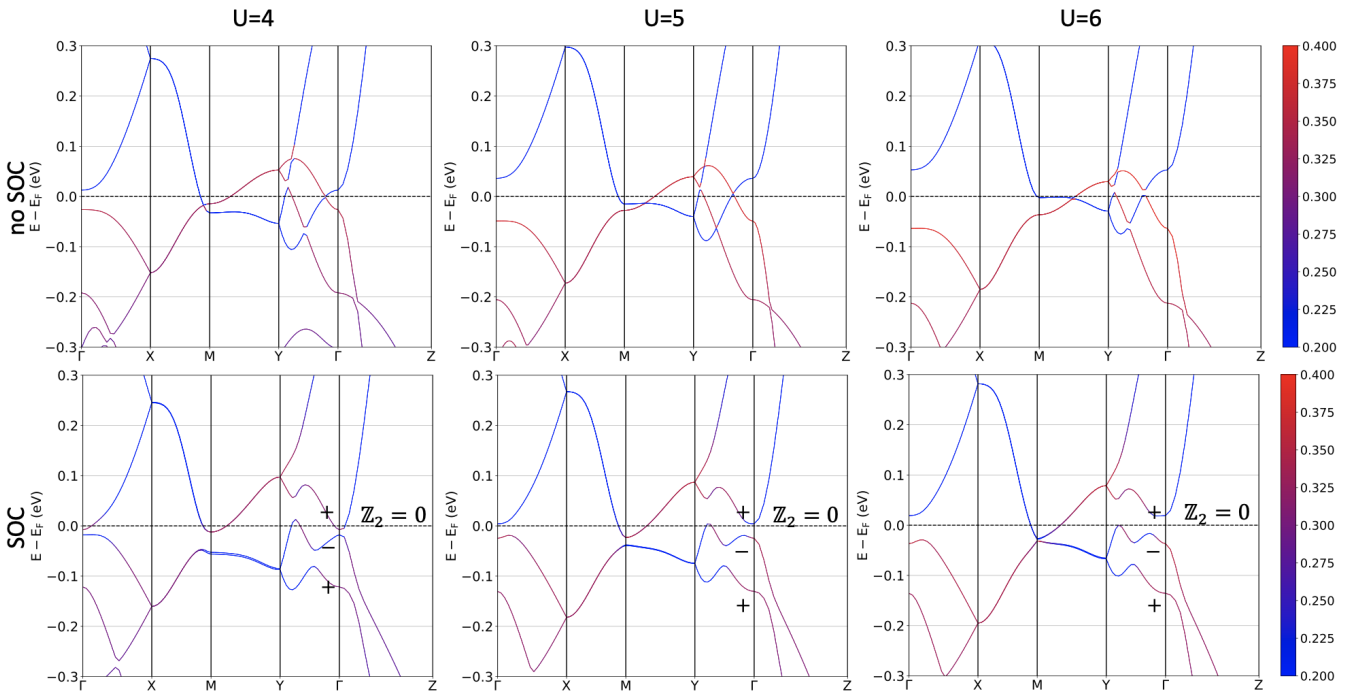

Supplementary Figure 2. Band structure of $Eu_5In_2Sb_6$ with and without SOC for $U = 4$eV, $U = 5$eV and $U = 6$eV in the A-type AFM configuration.

II. DEGENERACIES AND THE PARITY CRITERION

Here we show that only band inversions at Γ and Z can alter the axion $\mathbb{Z}_2$ index for a nonmagnetic material in the centrosymmetric SG 55. As explained below, this is related[4, 5] to the non-symmorphic nature of SG 55. Briefly, states at all time reversal invariant momenta (TRIM) except Γ and Z form 4-dimensional irreducible representations (irreps) for which the number of odd-parity states is fixed modulo four. In view of the Fu-Kane criterion for the strong $\mathbb{Z}_2$ index[6], band inversions at these TRIM points cannot change the $\mathbb{Z}_2$ index. Indeed, if n_K^- is the total number of odd-parity states at a given TRIM point, then the criterion can be expressed as

$$\prod_{\mathbf{k}\in\text{TRIM}} (-1)^{n_{\mathbf{k}}^-/2} \in \mathbb{Z}_2, \tag{1}$$

which remains unaffected when n_K^- is fixed modulo four.

We first explain how the 4-fold degeneracies arise. SG 55 can be regarded as generated by two glide mirrors $g_x = \{m_x|1/2, 1/2, 0\}$ and $g_y = \{m_y|1/2, 1/2, 0\}$ together with inversion I, all of which are good symmetries at all eight of the TRIM (see Table I). We can use the fact that $\{g_x, g_y\} = 0$ to show that if $|\psi_{\mathbf{k}}\rangle$ is an eigenstate of g_x, i.e., $g_x|\psi_{\mathbf{k}}\rangle = \alpha|\psi_{\mathbf{k}}\rangle$, then $g_x(g_y|\psi_{\mathbf{k}}\rangle) = -\alpha(g_y|\psi_{\mathbf{k}}\rangle)$. This implies $g_y|\psi_{\mathbf{k}}\rangle$, which has the same energy as $|\psi_{\mathbf{k}}\rangle$, is also an eigenstate of g_x with opposite eigenvalue. In addition, the Kramer's partners $T|\psi_{\mathbf{k}}\rangle$ and $Tg_y|\psi_{\mathbf{k}}\rangle$ will have g_x eigenvalues α^* and $-\alpha^*$ respectively. Taking into account that the g_x eigenvalues are $\alpha = \pm i(\pm 1)$ at $k_y = 0(\pi)$, we can conclude that Kramer's partners, which are necessarily orthogonal to each other, have opposite(same) eigenvalues at $k_y = 0(\pi)$. This then implies that $|g_y\rangle$, $T|\psi_{\mathbf{k}}\rangle$, $g_y|\psi_{\mathbf{k}}\rangle$ and $Tg_y|\psi_{\mathbf{k}}\rangle$ are mutually orthogonal at TRIM points where $k_y = \pi$ and they form 4D representations but is inconclusive when $k_y = 0$. Finally, note that we can apply the same line of thought after we swap the role of g_x and g_y leading to the conclusion that $|\psi_{\mathbf{k}}\rangle$, $T|\psi_{\mathbf{k}}\rangle$, $g_x|\psi_{\mathbf{k}}\rangle$ and $Tg_x|\psi_{\mathbf{k}}\rangle$ form 4D dimensional representations at TRIM points where $k_x = \pi$. Putting these together we conclude that TRIM points where either $k_x = \pi$ or $k_y = \pi$ admit representations of at least of degree four. In fact, using the computational tool BANDREP [7–9] of the Bilbao Crystallographic Server[10–12], we find that SG 55 admits only 4-dimensional irreps at these TRIM points.

Next we explain how the non-symmorphic symmetries constrain the inversion eigenvalues. Since

$$\begin{aligned} Ig_x &= g_x I e^{-ik_x + ik_y} \\ Ig_y &= g_y I e^{ik_x - ik_y} \end{aligned} \tag{2}$$

Supplementary Table I. Symmetry properties of glide mirrors g_x, g_y and inversion in SG 55.

Group Symmetry	g_x	g_y	I
Vector representation	$(\bar{x}+\frac{1}{2}, y+\frac{1}{2}, z)$	$(\bar{x}+\frac{1}{2}, y+\frac{1}{2}, z)$	$(\bar{x}, \bar{y}, \bar{z})$
Spinor representation	$-i\sigma_x$	$-i\sigma_y$	σ_0
Eigenvalues	$\alpha = \pm ie^{ik_y/2}$	$\beta = \pm ie^{ik_x/2}$	$\gamma = \pm 1$

depending on the TRIM point, inversion either commutes or anticommutes with g_x and g_y. In either case, g_x and g_y eigenstates are also inversion eigenstates. Considering the set of orthogonal states $\{|g_y\rangle, T|\psi_{\mathbf{k}}\rangle, g_y|\psi_{\mathbf{k}}\rangle, Tg_y|\psi_{\mathbf{k}}\rangle\}$ at the TRIM points with $k_y = \pi$, we observe that Kramer's partners share the same inversion eigenvalues, since they are real numbers, while states related by g_y will have opposite inversion eigenvalues when $k_x + k_y = \pi$, i.e., at the X,Y,U,T points, and same eigenvalues when $k_x + k_y = 2\pi$, i.e., at the S,R points. In the former case, the number of odd-parity states in each irreducible representation is 2 while in the latter is either 0 or 4. In either case band inversions can only change the parity count by 0 or 4 which does not affect the $\mathbb{Z}_2$ index.

III. DISPLACING THE In ATOM IN $Eu_5In_2Sb_6$

As we have seen in the main text displacing the In atom by modifying the y component of its Wyckoff position has the geometric effect of distorting the In-Sb tetrahedra by shortening the two In-Sb_1 bond and lengthening the In-Sb_2 and In-Sb_3 bonds.

The effect of the displacement on the band structure is shown in Supplementary Fig. 3. Here we focus on $k_z = 0$ plane, since $k_z = \pi$ remains gapped for all values of displacement, and the lowest conduction and highest valence bands, since they determined the topology and band gaps. For the actual structure, we see that the highest valence bands Supplementary Fig. 3(e) have primarily Sb character while the lowest conduction bands have primarily Eu character. This is what we should expect for a trivial insulator that follows the Zintl concept in which case we are at the limit of complete electron transfer for the Eu^{+10} cations to the $[In_2Sb_6]^{-10}$ polyanion.

Now as we progressively displace the In atoms, the character of the lowest conduction bands changes from Eu to In signaling that we are moving away from the limit of complete electron transfer. In this way, the energy of the lowest conduction bands decreases and that of the highest valence bands increases. The increased overlap causes a band inversion at Γ when SOC is included which makes the $\mathbb{Z}_2$ index non-trivial.

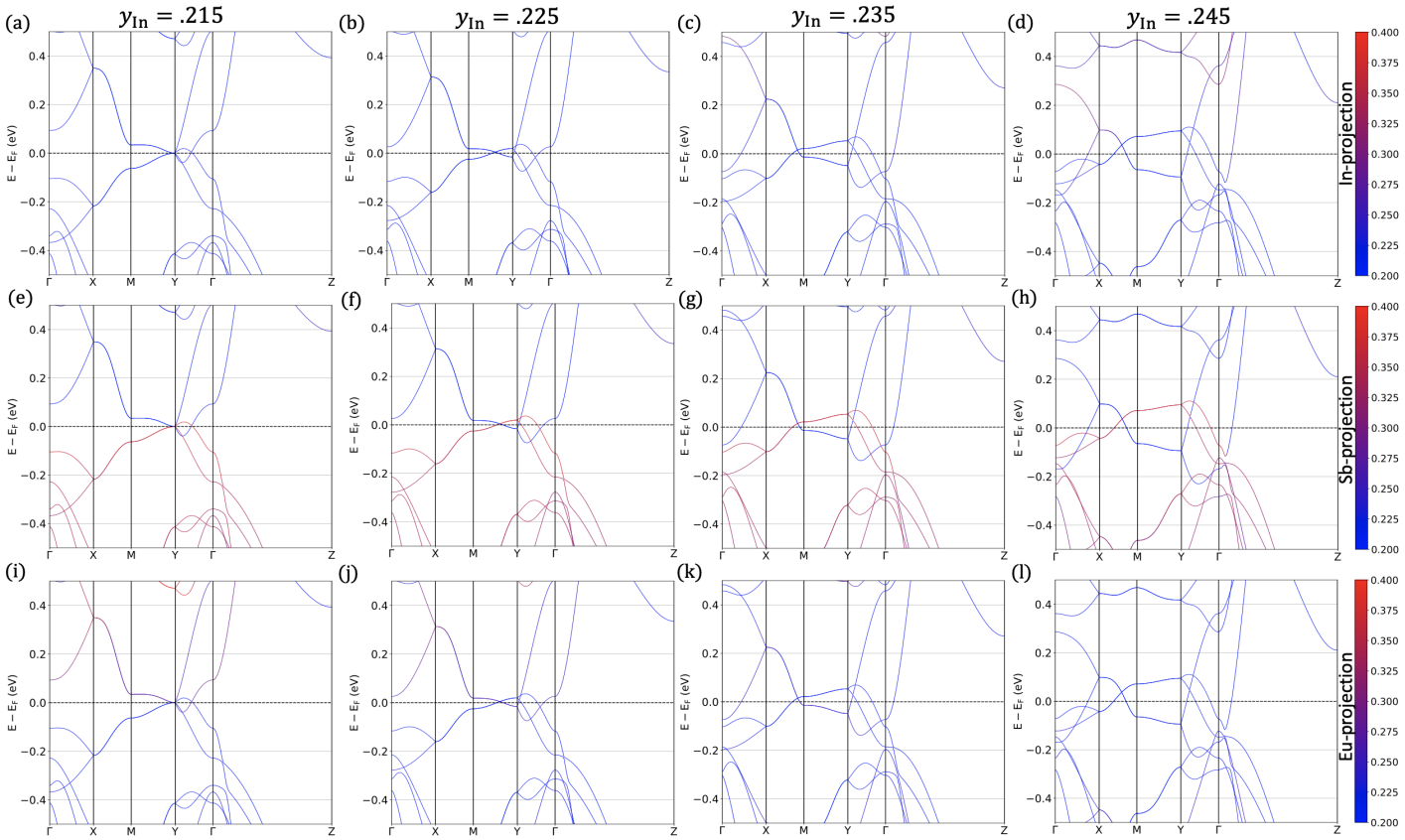

Supplementary Figure 3. Band structures without SOC for different values of the y-component of the In atom's Wyckoff position. From the left to right the band structures interpolate between the actual $y_{In} = .2149$ and the one that was reported in Rosa *et al.* [2] $y_{In} = 2419$. The three rows, correspond to projections on the In (a)-(d), Sb (e)-(h) and Eu (i)-(l) atoms respectively.

IV. CHANGING THE TOPOLOGY OF $Eu_5In_2Sb_6$ THROUGH THE APPLICATION OF STRAIN

Here we show that applying compressive uniaxial strain along c or expansive epitaxial strain in the $a-b$ plane has a similar effect as displacing the In atom. In particular, Supplementary Fig. 4 shows the overlap between conduction and valence bands increases when either of these structural perturbations is applied, indicating that the compound is moving away from the CET limit. For extreme values of, around $\sim 10\%$ compressive uniaxial strain or $\sim 10\%$ expansive epitaxial strain, the $\mathbb{Z}_2$ index changes. However, this not only impractical to realize due to the large magnitude of strain but the increased bandwidth of the strained bands results in metallic states.

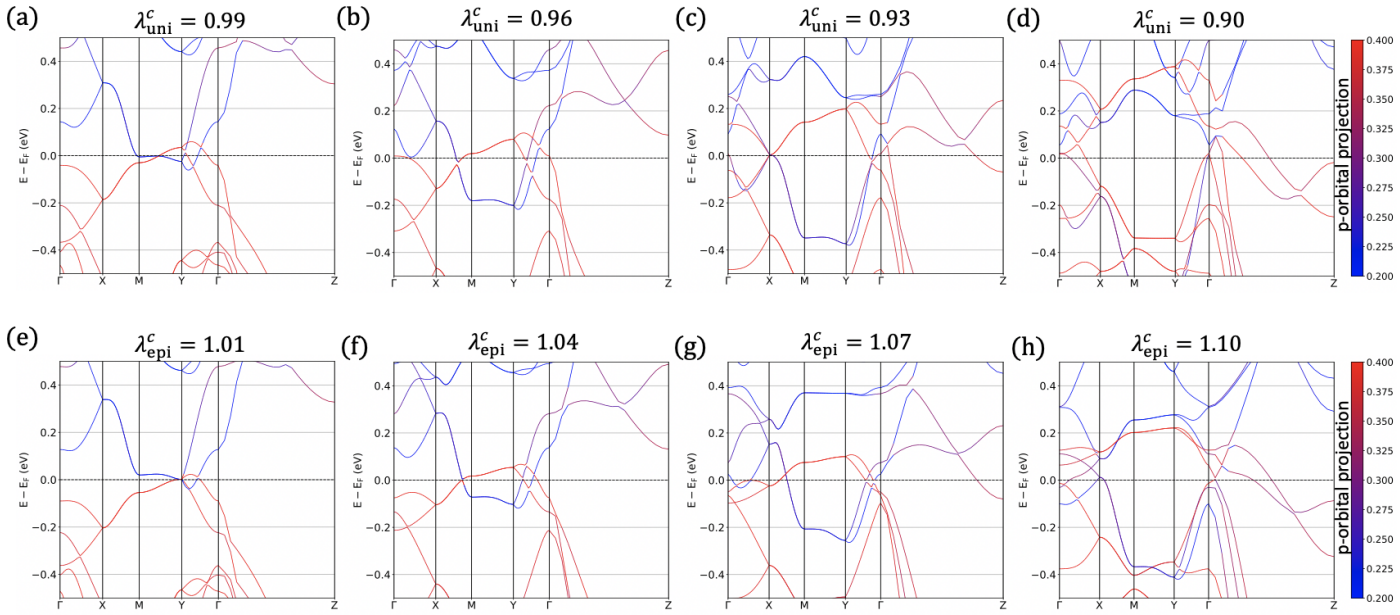

Supplementary Figure 4. Band structures without SOC for different values of uniaxial (a)-(d) and epitaxial (e)-(h) strain. The color mapping indicates the p-orbital projection of the states.

V. STABLE Ga AND Tl SUBSTITUTED STRUCTURES

Starting from $Eu_5In_2Sb_6$ we substitute In with Ga or Tl and perform relaxation of the substituted structures (both the internal coordinates and lattice constants). We find that the system remains in SG 55. The structural parameters for $Eu_5Ga_2Sb_6$ and $Eu_5Tl_2Sb_6$ are given in Supplementary Tables I,II. To see whether the structures are dynamically stable, we calculate the phonon spectrum, Supplementary Fig. 5. Since the spectrum are positive this indicates that the structures are stable and could be synthesized.

Supplementary Table II. Structure parameters of $Eu_5Ga_2Sb_6$

Atom	x	y	z	Site	Sym.
Eu_1	0.33118	0.02082	0.00000	4g	..m
Eu_2	0.00000	0.00000	0.00000	2a	..2/m
Eu_3	0.91044	0.75223	0.00000	4g	..m
Sb_1	0.16526	0.82065	0.00000	4g	..m
Sb_2	0.15615	0.09174	0.50000	4h	..m
Sb_3	0.51984	0.09902	0.50000	4h	..m
Ga_1	0.32645	0.21143	0.50000	4h	..m

Supplementary Table III. Structure parameters of $Eu_5Tl_2Sb_6$

Atom	x	y	z	Site	Sym.
Eu_1	0.32862	0.02364	0.00000	4g	..m
Eu_2	0.00000	0.00000	0.00000	2a	..2/m
Eu_3	0.91530	0.75173	0.00000	4g	..m
Sb_1	0.16890	0.83477	0.00000	4g	..m
Sb_2	0.14766	0.09124	0.50000	4h	..m
Sb_2	0.53550	0.09370	0.50000	4h	..m
Tl_1	0.33215	0.21692	0.50000	4h	..m

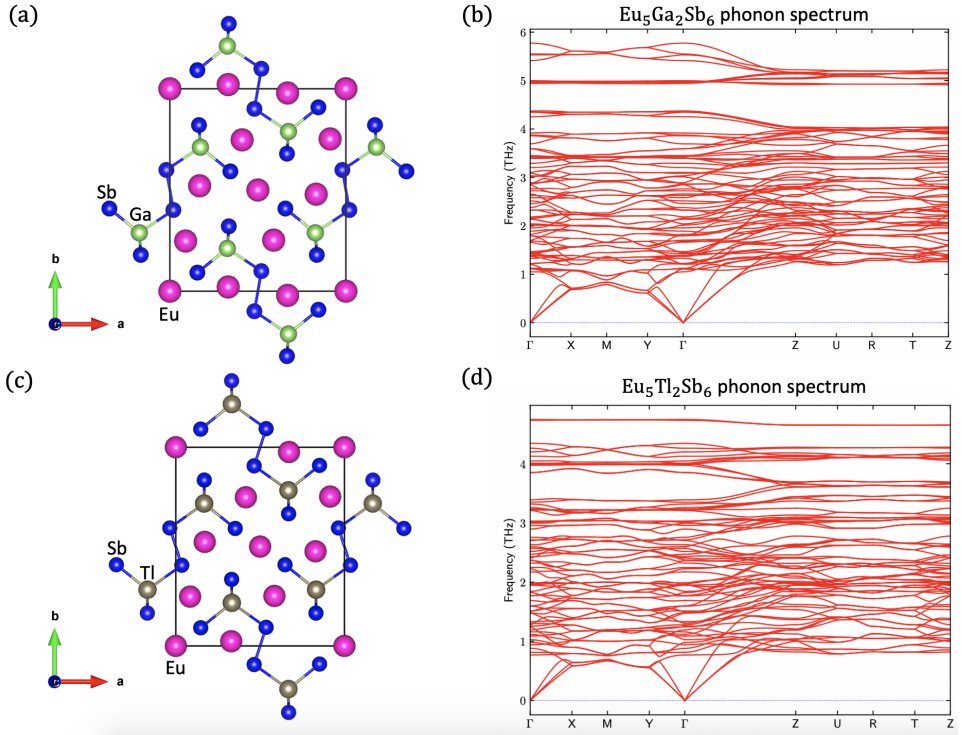

Supplementary Figure 5. (a),(b) Crystal structure and phonon spectrum for $Eu_5Ga_2Sb_6$ (c),(d) Same for $Eu_5Tl_2Sb_6$.

VI. BAND GAP ENGINEERING USING EPITAXIAL STRAIN

In the main text we showed that uniaxial strain can be used to control the direct and indirect gaps of $Eu_5In_2Bi_6$. Here we present a similar analysis for epitaxial strain in $Eu_5In_2Bi_6$. Supplementary Fig. 6(a),(b) show that epitaxial strain with $\lambda^c_{\rm epi} < 1.00$ or $\lambda^a_{\rm epi} > 1.00$ enhance the direct and indirect gaps.

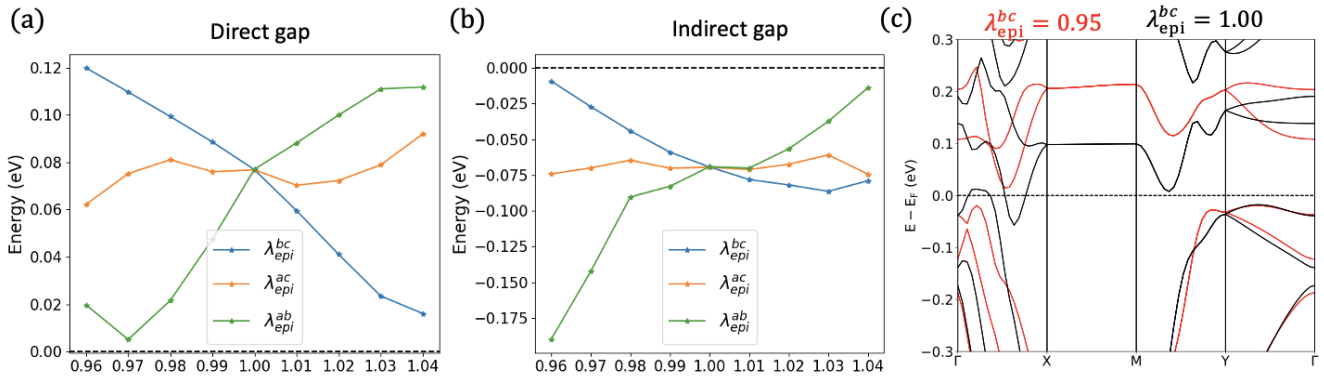

Supplementary Figure 6. Effect of uniaxial strain on (a) direct and (b) indirect gap. (c) Comparison between band structures with $\lambda^{bc}_{\rm uni} = 1.00$ and $\lambda^{bc}_{\rm uni} = 0.95$.

[1] Y. Xu, Z. Song, Z. Wang, H. Weng, and X. Dai, Phys. Rev. Lett. **122**, 256402 (2019).
[2] P. Rosa, Y. Xu, M. Rahn, J. Souza, S. Kushwaha, L. Veiga, A. Bombardi, S. Thomas, M. Janoschek, E. Bauer, M. Chan, Z. Wang, J. Thompson, N. Harrison, P. Pagliuso, A. Bernevig, and F. Ronning, npj Quantum Materials **5**, 52 (2020).
[3] M. Yu, S. Yang, C. Wu, and N. Marom, npj Computational Materials **6**, 180 (2020).
[4] Y. Chen, H.-S. Kim, and H.-Y. Kee, Phys. Rev. B **93**, 155140 (2016).
[5] B. J. Wieder, B. Bradlyn, Z. Wang, J. Cano, Y. Kim, H.-S. D. Kim, A. M. Rappe, C. L. Kane, and B. A. Bernevig, Science **361**, 246 (2018), https://www.science.org/doi/pdf/10.1126/science.aan2802.
[6] L. Fu and C. L. Kane, Phys. Rev. B **76**, 045302 (2007).
[7] B. Bradlyn, L. Elcoro, J. Cano, M. G. Vergniory, Z. Wang, C. Felser, M. I. Aroyo, and B. A. Bernevig, Nature **547**, 298 (2017).
[8] M. G. Vergniory, L. Elcoro, Z. Wang, J. Cano, C. Felser, M. I. Aroyo, B. A. Bernevig, and B. Bradlyn, Phys. Rev. E **96**, 023310 (2017).
[9] L. Elcoro, B. Bradlyn, Z. Wang, M. G. Vergniory, J. Cano, C. Felser, B. A. Bernevig, D. Orobengoa, G. de la Flor, and M. I. Aroyo, Journal of Applied Crystallography **50**, 1457 (2017).
[10] M. I. Aroyo, A. Kirov, C. Capillas, J. M. Perez-Mato, and H. Wondratschek, Acta Crystallographica Section A **62**, 115 (2006).
[11] M. I. Aroyo, J. M. Perez-Mato, C. Capillas, E. Kroumova, S. Ivantchev, G. Madariaga, A. Kirov, and H. Wondratschek, Zeitschrift für Kristallographie - Crystalline Materials **221**, 15 (2006).
[12] M. I. Aroyo, J. Perez-Mato, D. Orobengoa, E. Tasci, G. De la Flor Martin, and A. Kirov, Bulgarian Chemical Communications **43**, 183 (2011).